JOURNAL OF FORENSIC SCIENCES

J Forensic Sci, September 2012, Vol. 57, No. 5
doi: 10.1111/j.1556-4029.2012.02144.x
Available online at: onlinelibrary.wiley.com

CASE REPORT

PATHOLOGY/BIOLOGY

Patricia M. Flach,[1,2] M.D.; Steffen G. Ross,[1] M.D.; Stephan A. Bolliger,[1] M.D.; Garyfalia Ampanozi,[1] M.D.; Gary M. Hatch,[1] M.D.; Corinna Schön,[1] M.D.; Michael J. Thali,[1] M.D.; and Tanja Germerott,[1] M.D.

Massive Systemic Fat Embolism Detected by Postmortem Imaging and Biopsy*

ABSTRACT: Postmortem computed tomography (pmCT) and pmCT angiography (pmCTA) provide a minimally invasive method to determine the cause of death. Postmortem image-guided biopsy allows for precise sampling of histological specimens. This case study describes the findings of lethal systemic fat embolism (FE) on whole-body unenhanced pmCT, pmCTA, and image-guided biopsy, with autopsy and histopathologic correlation. Unenhanced pmCT revealed a distinct fat level on top of sedimented layers of corpuscular blood particles and serum in the arterial system and pulmonary trunk. Subsequent pmCTA showed reproducible results, and image-guided biopsy confirmed fatal FE. pm CT/pmCTA combined with image-guided biopsy established the cause of death as right heart failure as a result of systemic fatal FE prior to autopsy. All imaging findings were consistent with traditional autopsy and histological specimens. This unique case demonstrates new imaging findings in massive, fatal FE and highlights that postmortem imaging, supplemented by image-guided biopsy, may detect the cause of death prior to traditional autopsy.

KEYWORDS: forensic science, fat embolism, systemic fat embolism, computed tomography, virtopsy, postmortem imaging, computed tomography, postmortem computed tomography angiography

The pathophysiology of fat embolism (FE) is poorly understood and is presumably based on two mechanisms: mechanical obstruction of the pulmonary vasculature by fat globules (that may leak through the lung capillaries into the systemic circulation) and toxic changes in the endothelium as a result of production of free fatty acids (1–4). This predominantly impacts organs such as the brain, kidneys, and myocardium and may lead to death (2). FE has been recognized for over a century and is an important sequel to trauma (5,6). Most commonly, FE is described after major trauma-associated long bone fracture owing to intravasation of bone marrow and fat into the venous blood system (5). The development of clinical symptoms correlates with the amount of FE in the lungs or the major circulation. However, numerous other pathogeneses such as metabolic syndrome, lipid transport disorders, steroid therapy, indirect cardiac massage, soft-tissue injury, surgical intervention on fatty tissue, major burns, hip or knee replacement, renal failure, hemoglobinopathy, pancreatitis, infection, tumors, barotrauma, blood transfusion, intravenous nutrition, fatty liver, acute pancreatitis, and liposuction must be taken into account as potential etiologies of FE (7–11). Pulmonary, cerebral, or cutaneous symptoms usually occur 12–24 h after trauma, and radiographic signs are typically seen 12 h after the onset of clinical symptoms (1,12). FE presents on antemortem imaging most commonly with hypodense, low attenuation filling defects in the lung arteries and may potentially appear as ground-glass opacity and consolidation in the lung parenchyma (13–16).

Postmortem imaging provides a minimally invasive method to examine decedents for causes of deaths (17–19). Unenhanced postmortem computed tomography (pmCT) offers details of general pathologies of the whole body such as traumatic injury patterns of the osseous system, fatal air embolism, the course of stab and gunshot wounds, dental identification, and localization of foreign materials (e.g., projectiles) or other gross lesions. However, little can be said about the status of the vascular system owing to a lack of contrast in unenhanced pmCT. Recently established pmCT angiography (pmCTA) can be performed to provide a precise display of vascular and tissue lesions (20–22). Image-guided tissue sampling can enhance macroscopic image information to offer microscopic detail (23,24). The purpose of our case study is to describe the findings of lethal systemic FE on unenhanced pmCT, pmCTA, and image-guided lung biopsy, with correlation to conventional autopsy and histopathology.

Materials and Methods

Case History

An 89-year-old woman (167 cm, 52 kg) stumbled upon an apple while having a walk and fell on her left hip. Directly after the fall, she was transferred to a nearby emergency unit and diagnosed with a fracture of the left femoral neck. The patient was under long-term therapeutic anticoagulation for a history of atrial fibrillation. In the course of treatment, anticoagulation was discontinued and antidote (vitamin K) was administered. No disorder of lipid metabolism/transport or renal failure was known in the patient`s history. The patient was on no other prescription medication. Aside from

[1]Centre for Forensic Imaging and Virtopsy, Institute of Forensic Medicine, University of Bern, Buehlstrasse 20, 3012 Bern, Switzerland.
[2]Department of Neuroradiology, Inselspital Bern, University of Bern, 3010 Bern, Switzerland.

*Presented at the 63rd Annual Meeting of the American Academy of Forensic Sciences, February 21–26, in Chicago, IL.

Received 3 Feb. 2011; and in revised form 23 May 2011; accepted 14 Aug. 2011.

the atrial fibrillation, she had no other cardiac history. Surgical history revealed a previously implanted gamma nail in the right hip, and she presented with an old healed fracture of the inferior and superior pubic ramus as a result of a prior trauma years ago.

One day after the initial trauma, the patient consented to surgical intervention after prior preoperative patient briefing including the risk of potential cardiac arrest. Laboratory tests and preoperative exams revealed no additional potential risks for surgery other than age and known atrial arrhythmia. During placement of the cemented endo-prosthesis, cardiac arrest occurred. Resuscitation attempts were unsuccessful. It is unknown whether the prosthesis was reamed or broached.

Imaging and Vascular Access

The ethics committee of the university approved this study. The body underwent whole-body pmCT (Somatom Emotion 6; Siemens, Erlangen, Germany) with subsequent minimally invasive cannulation via an unilateral inguinal incision (16Fr artery; 20Fr vein; Medtronic, Fridley, MN) 19.5 h after time of death as already described by Ross et al. (22). Raw data acquisition was performed with the following settings: collimation 6 × 1 mm whole body; unenhanced pmCT with 130 kV, 160 mAs; and pmCTA with 110 kV, 160 mAs. Calculation of soft-tissue/bone-weighted algorithm (5 mm/1.25 mm) was standard. A contrast media mixture of poly ethylene glycol (PEG 200; Schaerer & Schlaepfer AG, Rothrist, Switzerland) and Iopentol (Imagopague 300; Amersham Health, Wädenswil, Switzerland) was administered (22). pm CTA was then performed with an arterial and venous injection using a modified heart–lung machine (HL20; Maquet, Gossau, Switzerland). The body was moved from supine to prone position, and the thorax was then scanned again to overcome position-dependent filling defects. Thereafter, the body was turned back to the supine position and scanned again, 50 min after the initial unenhanced scan, to reproduce gravity and sedimentation-dependent effects.

Image-Guided Biopsy

After pmCT and pmCTA, four image-guided percutaneous needle biopsy specimens of the bilateral central and peripheral lungs were obtained by the radiologist. Additional biopsy of potential central pulmonary thromboembolism was obtained to differentiate between antemortem pulmonary thromboembolism and postmortem clotting (cruor) (23). Puncture sites were marked externally for orientation during autopsy. Biopsies were performed with a Bard Magnum biopsy gun and a 14G UltraCORE Biopsy Needle (Inter.V; all biopsy equipment from Bard Biopsy Systems, Tempe, AZ). The harvested specimens were stained with Oil Red to detect FE and analyzed by a board-certified forensic pathologist.

Autopsy

Routine traditional autopsy with dissection of all three body cavities and sampling of tissue specimens (such as double-edged knife specimens of the lungs stained with Sudan Red) were performed 40.5 h after death.

Results

Imaging and Biopsy

Initial unenhanced pmCT revealed a distinct fat level, consistent with massive FE, on top of sedimented layers of corpuscular blood particles and serum in the systemic circulation (namely, right ventricle and atrium, ascending aorta, brachiocephalic trunk, left common carotid artery, superior mesenteric artery) and the pulmonary trunk (Fig. 1). The fat layer was detectable macroscopically only in larger-diameter vessels and in the anterior aspect of vessels when scanned in the supine position.

Hounsfield unit (HU) measurements revealed −40 to −90 HU in this intravascular fat-equivalent layer, which was almost equivalent to the typical HU of mediastinal fat −60 to −100 HU. On the Hounsfield scale, fat would typically be represented by 0 to −100 HU. Intravascular gas would result in *c.* −1000 HU on the HU scale and appear as a typical round to oval gas bubble. Intraluminal fat has a broad-based layer on top of serum and sedimented corpuscular blood particles owing to its physical characteristics.

Subsequent pmCTA was performed to exclude other potential causes of death and showed no clotting to suggest pulmonary thromboembolism. However, central presumed postmortem clotting

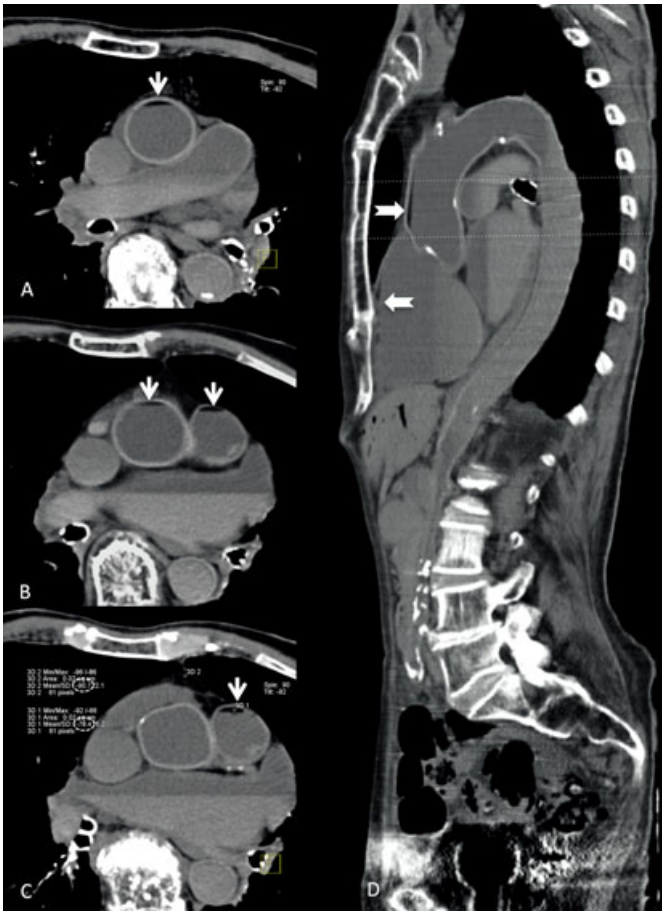

FIG. 1—*(A–C) Axial slices [all unenhanced postmortem computed tomography (pmCT)] at the level of the ascending aorta and the pulmonary artery (D). (A) Note the distinct, broad based fat layer on top of the serum in the ascending aorta (white short arrow). (B) The subtle fat layer (white short arrow) is present on top of the serum in the ascending aorta (major circulation) and the pulmonary artery (minor circulation). Note the distinct level of the corpuscular blood particles (bright grey layer) and the serum (dark grey layer) in the dependent portion of the vessel when in the supine position. (C) Hounsfield unit (HU) for fat typically measures from 0 to −100 on the HU scale. The fat layer (dark grey layer, 3D 1) is −78 HU, note the similar measurement of the mediastinal fat (3D 2) with −90 HU. (D) The sagittal reconstruction shows the three layered intravascular components: fat layer (bold white arrow), corpuscular blood particles (bright grey layer), and serum (dark grey layer).*

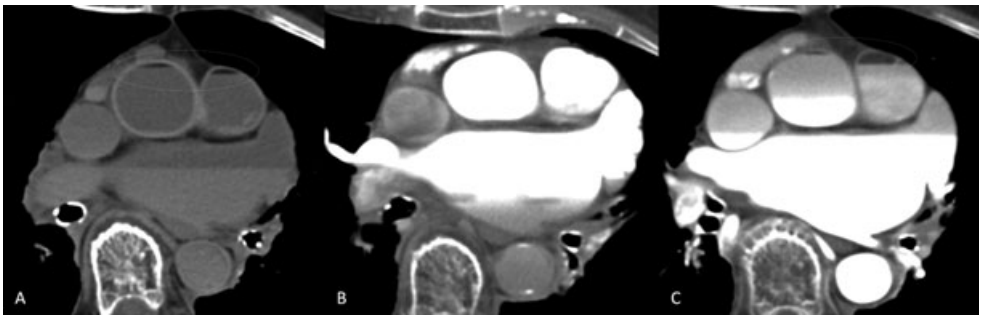

FIG. 2—*Axial slices at the level of the ascending aorta, the pulmonary artery and the left atrium. (A) Unenhanced postmortem computed tomography (pmCT). Note the clear line of sedimented corpuscular particles (bright grey layer) in the dependent posterior position when scanned in supine position. Above, the blood serum (darker grey layer) can be seen. Note the distinct fat layer in the pulmonary trunk and ascending aorta (white circle). (B) pmCTA. Intermingled intravascular components and contrast media mixture (prone position). (C) pmCTA scan 50 min after unenhanced pmCT (supine position) with reproducible triple layer consisting of sedimenting contrast media mixture, blood (serum and corpuscular particles with initial sedimentation), and fat (white circle).*

was present in the pulmonary artery. Image-guided biopsy confirmed postmortem clotting and proved that no antemortem pulmonary thromboembolism was present.

During pmCTA of the thorax in the supine and thereafter in the prone position, the three intravascular components, fat layer, blood (corpuscular blood particles and serum), and contrast media mixture, intermingled (Fig. 2). After turning the decedent back to supine position and giving the intravascular components time (50 min after unenhanced scan) to sediment, the triple-layered intravascular findings were reproducible.

In addition, images confirmed the correctly implanted total endoprosthesis of the left hip and the reported gamma nail of the right hip with an ipsilateral, old healed fracture of the inferior and superior pubic rami (Fig. 3). Besides that, a dilated right atrium and minor coronary sclerosis were noted. No pulmonary changes such as ground-glass opacity, consolidation, thickening of interlobular walls, pleural effusion, or lividity were present. Unenhanced pmCT showed no hypodense artery sign correlating to intracranial FE (25).

pmCTA allowed for a proper evaluation of the vascular system and the soft tissues, which augmented the findings from unenhanced pmCT. There were no vascular ruptures, dissections, aneurysms, or lesions of parenchymal organs on pmCTA. Assessment of the whole-body images on pmCT and pmCTA showed no other causes of death than massive systemic FE. Histology of the lung biopsies demonstrated severe FE (Grade IV, according to the system of Mason, Grade III, according to the system of Falzi) (Fig. 5) (26,27).

Autopsy and Histology

External inspection showed a normal-appearing operative incision on the left hip. Superficial abrasions were noted on her left elbow and left tibia, as a result of the fall. There was no edema

FIG. 3—*Volume reconstruction of the pelvis and femoral bones with color-coded foreign objects (blue). On the right a previously implanted gamma-nail, on the left the newly implanted endo-prosthesis. Note the stapling of the operation access.*

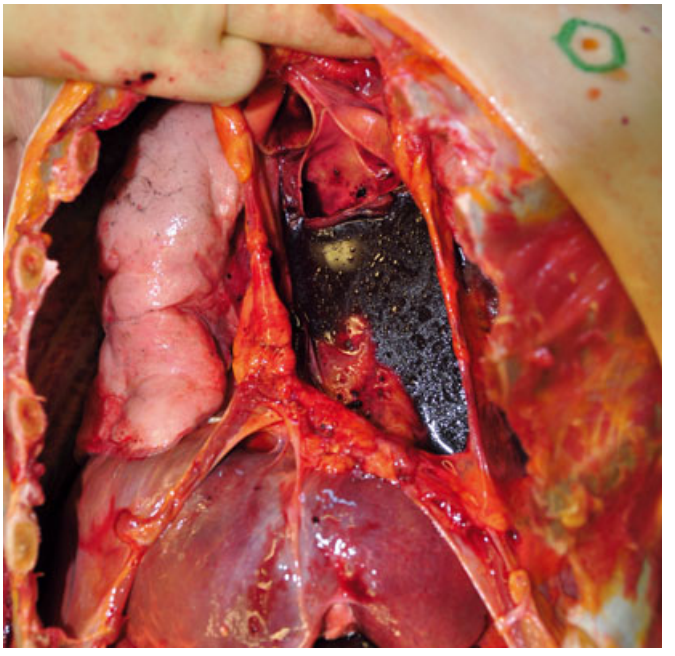

FIG. 4—*Note the macroscopically visible fat drops within the thoracic cavity. The image-guided puncture site is marked externally for orientation during autopsy (green circle).*

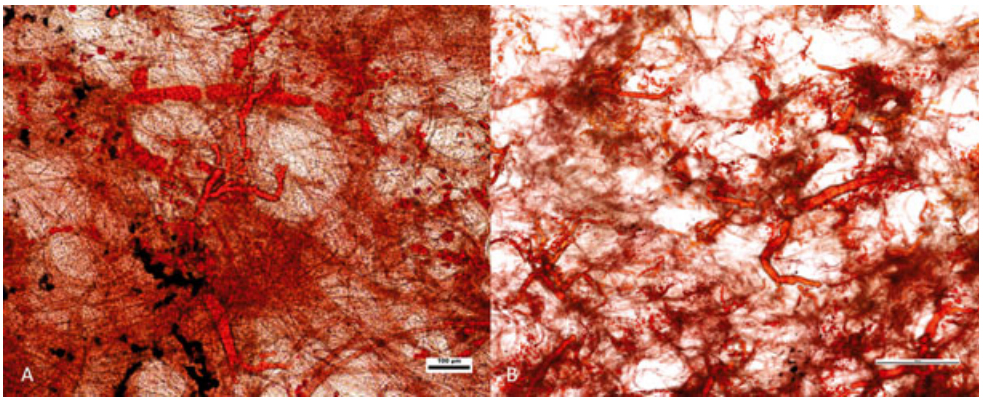

FIG. 5—*Both images show fat embolism Grade IV (Mason) or Grade III (Falzi). (A) Image-guided biopsy specimen (100 μm scale). (B) Double-edged knife specimen obtained during autopsy (500 μm scale).*

with side differences found on the lower extremities. Dissection of the surgical access showed a typical postinterventional hematoma of the soft tissue. The forensic dissection revealed no patent foramen ovale, pulmonary thromboembolism, myocardial infarction, or other cause of death. No petechial rash or kidney or brain parenchymal changes were visible, as might be expected with systemic FE. Histology of these organs added no additional findings. The heart showed slight right atrial hypertrophy with no pulmonary congestion/edema, but minor coronary sclerosis. During autopsy, fat drops were visible macroscopically in the thoracic cavity (Fig. 4). Autopsy with histology of the double-edged knife specimens determined the cause of death as right heart failure owing to FE (Grade IV, Mason or Grade III, Falzi) as a result of the implantation of a cemented total hip prosthesis (Fig. 5) (26,27).

Discussion

Both image-guided biopsy and histopathologic specimens obtained during autopsy confirmed the findings of pmCT/CTA demonstrating severe FE, leading to right heart failure as the cause of death. Autopsy findings confirmed the conclusions drawn from imaging and biopsy.

Further evaluation of this case showed that there were no suggestions for cholesterol embolism, for example, triggered by anticoagulation. There were no other predisposing factors for FE such as multi-injury at one time, massive soft-tissue injury, obesity, diabetes mellitus, metabolic syndrome, intravenous lipid hyperalimentation, burns, corticosteroid therapy, sickle cell disease (causing bone infarcts), fatty liver, acute pancreatitis, renal failure, infection, osteomyelitis, liposuction, bone marrow biopsy, blood transfusion, or tumor (5–9,12,13). Intraoperative documentation stated that no external cardiac massage had taken place except defibrillation (10,11). It could not be evaluated whether the endo-prosthesis had been reamed or broached as the reaming technique is known to cause more FE complications owing to bone marrow compression (28,29). The patient showed no clinical symptoms according to Gurd's (12) criteria such as petechial hemorrhages, dyspnea, tachycardia, anxiety, unconsciousness, or retinal signs prior to surgery to suggest that the onset of FE occurred preoperatively.

To the best of our knowledge, this is the first description of these unique systemic postmortem imaging findings. FE with intravascular fat layers on imaging is a rare finding, but may be increasingly described as pmCT exams are performed as a more frequent part of routine forensic examination. A recent case study by Filograna et al. (24) showed promising results in detecting pulmonary FE on pmCT combined with image-guided biopsy in a case of autopsy refusal. Nonetheless, the image-guided biopsy revealed FE, while the imaging showed only indirect pulmonary changes with no intravascular fat layers (24). On other reports of antemortem scans, FE has been described as a subtle imaging finding, usually located in peripheral or paracentral lung vessels (13–16), but has never been reported as a systemic finding on imaging. This is probably based on the facts that FE of such an extent is incompatible with life, the volume of FE is lower in survivors and tends to be located in the peripheral or paracentral pulmonary arteries, and blood circulation homogenizes blood components in the antemortem scan and does not allow for layered findings. We hypothesize that the lack of accompanying pulmonary changes and abnormalities in the kidney's glomeruli, the myocardial interfibers, the white matter of the brain, and the absence of petechial skin hemorrhages in this case is explicable by pressure-assisted ventilation during surgery and the sudden onset of the massive FE with no time to evolve typical ground-glass patterns, consolidation or even pulmonary edema of the lung, or alterations of the kidney, brain, or myocardium (1). However, pulmonary and parenchymal changes owing to FE are not obligatory to the diagnosis of FE and are yet not frequently seen (2,14,16).

Conclusions

In this case, the diagnosis of fatal systemic FE was able to be determined prior to subsequent autopsy. This case description lends further support toward the increased use of minimally invasive virtual autopsy as a potential replacement for traditional autopsy in selected cases and when the cause of death is clearly defined by imaging and image-guided biopsy (30).

References

1. Han D, Lee KS, Franquet T, Müller NL, Kim TS, et al. Thrombotic and nonthrombotic pulmonary arterial embolism: spectrum of imaging findings. Radio Graphics 2003;23:1521–39.
2. Knight B, Saukko P. Complications of injury. In: Knight B, Saukko P, editors. Knight's forensic pathology. London, UK: Edward Arnold Ltd, 2004;340–4.
3. Böcker W, Denk H, Heitz PU. Pathologie. In: Böcker W, Denk H, Heitz PU, editors. München, Wien, Baltimore, MD: Urban & Schwarzenberg, 1997;214.
4. Huber-Lang M, Brinkmann A, Straeter J, Beck A, Gauss A, Gebhard F. An unusual case of early fulminant post-traumatic fat embolism syndrome. Anaesthesia 2005;60:1141–3.

5. Tanner B, Jones J, Cople S, Davison P. Fat embolization in trauma facilities. Ann Emerg Med 1990;19:57.
6. Bergmann E. *Ein fall tödlicher fettembolie*. Berliner Medizinische Wochenschrift 1873;10:385.
7. Woo OH, Yong HS, Oh Y-W, Shin BK, Kim HK, Kang E-Y. Experimental pulmonary fat embolism: computed tomography and pathologic findings of the sequential changes. J Korean Med Sci 2008;23:691–9.
8. Saad RA, Fahmy AA, Ahmed MH. Fatal fat embolism complicating cemented total knee replacement: another manifestation of the metabolic syndrome? Arch Orthop Trauma Surg 2007;127:387–9.
9. Fulde GW, Harrison P. Fat embolism—a review. Arch Emerg Med 1991;8:233–9.
10. Steiner I, Klempírová A. Indirect cardiac massage as a cause of pulmonary fat embolism. Cesk Patol 1990;26(2):109–11.
11. Scherer G, Dick W. *Fettembolie. Eine ernste komplikation der reanimation?* H.- Notfall & Rettungsmedizin 1999;2:134–40.
12. Gurd AR. Fat embolism: an aid to diagnosis. J Bone Joint Surg Br 1970;52(4):732–7.
13. Huang BK, Monu JUV, Wandtke J. Pulmonary fat embolism after pelvic and long bone fractures in a trauma patient. Emerg Radiol 2009;16:407–9.
14. Ravenel JG, Heyneman LE, Page McAdams H. Computed tomography diagnosis of macroscopic pulmonary fat embolism. J Thorac Imaging 2002;17:154–6.
15. Arakawa H, Kurihara Y, Nakajima Y. Pulmonary fat embolism syndrome: CT findings in six patients. J Comput Assist Tomogr 2000;24(1):24–9.
16. Nucifora G, Hysko F, Vit A, Vasciaveo A. Pulmonary fat embolism: common and unusual computed tomography findings. J Comput Assist Tomogr 2007;31:806–7.
17. Thali MJ, Yen K, Schweitzer W, Vock P, Boesch C, Ozdoba C, et al. Virtopsy, a new imaging horizon in forensic pathology: virtual autopsy by postmortem multislice computed tomography (MSCT) and magnetic resonance imaging (MRI)—a feasibility study. J Forensic Sci 2003;48(2):386–403.
18. Thali MJ, Dirnhofer R. Intravital versus postmortem imaging. In: Thali MJ, Dirnhofer R, Vock P, editors. The virtopsy approach: 3D optical and radiological scanning and reconstruction in forensic medicine. Boca Raton, FL: CRC Press, Taylor & Francis Group, 2009;145–6.
19. Rutty GN, Morgan B, O'Donnell C, Leth PM, Thali M. Forensic institutes across the world place CT or MRI scanners or both into their mortuaries. J Trauma 2008;65(2):493–4.
20. Grabherr S, Djonov V, Yen K, Thali MJ, Dirnhofer R. Postmortem angiography: review of former and current methods. AJR Am J Roentgenol 2007;188(3):832–8.
21. Jackowski C, Persson A, Thali MJ. Whole body postmortem angiography with a high viscosity contrast agent solution using poly ethylene glycol as contrast agent dissolver. J Forensic Sci 2008;53(2):465–8.
22. Ross S, Spendlove D, Bolliger S, Christe A, Oesterhelweg L, Grabherr S, et al. Postmortem whole-body CT angiography: evaluation of two contrast media solutions. AJR Am J Roentgenol 2008;190(5):1380–9.
23. Bolliger SA, Filograna L, Spendlove D, Thali MJ, Dirnhofer S, Ross S. Postmortem imaging-guided biopsy as an adjuvant to minimally invasive autopsy with CT and postmortem angiography: a feasibility study. AJR Am J Roentgenol 2010;195:1051–6.
24. Filograna L, Bolliger SA, Spendlove D, Schön C, Flach PM, Thali MJ. Diagnosis of fatal pulmonary fat embolism with minimally invasive virtual autopsy and post-mortem biopsy. J Leg Med 2010;12:233–7.
25. Lee TC, Bartlett ES, Fox AJ, Symons SP. The hypodense artery sign. AJNR Am J Neuroradiol 2005;26:2027–9.
26. Mason JK. Pulmonary fat and bone marrow embolism as an indication of ante-mortem violence. Med Sci Law 1968;8:200–6.
27. Falzi G, Henn R, Spann W. On pulmonary fat embolism after injuries with different periods of survival. Munch Med Wochenschr 1964;106:978–81.
28. DiGiovanni CW, Garvin KL, Pellicci PM. Femoral preparation in cemented total hip arthroplasty: reaming or broaching? J Am Acad Orthop Surg 1999;7(6):349–57.
29. Giannoudis PV, Tzioupis C, Pape H-C. Fat embolism: the reaming controversy. Injury Int J Care Injured 2006;37S:S50–8.
30. O'Donnell C, Woodford N. Post-mortem radiology—a new sub-speciality? Clin Radiol 2008;63(11):1189–94.

Additional information and reprint requests:
Patricia M. Flach, M.D.
Centre for Forensic Imaging and Virtopsy
Institute of Forensic Medicine
University of Bern
Buehlstrasse 20
3012 Bern
Switzerland
E-mail: patricia.flach@irm.uzh.ch